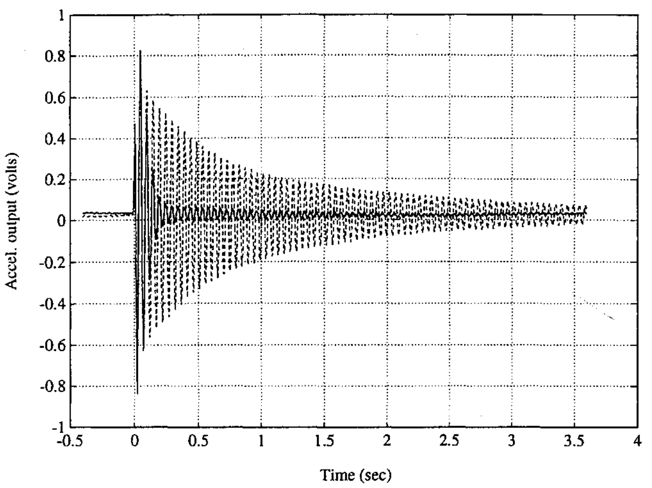

Fig. 3 Closed-loop response displaying residual vibration (solid line) compared to open loop (dashed line).

the self-sensing methods depends on proper impedance matching of elements to cancel out the control voltage, this nonlinearity is of crucial importance.

The limit cycle behavior of Fig. 3 can also be explained by nonlinearities of the system. Hysteresis, control voltage bleed through, and noise are the three most prevalent causes of suboptimum closed-loop performance for this project. The latter two phenomena were ruled out as causes of the limit cycle behavior after performing numerous simulations. Hysteresis is difficult to simulate but is known to cause limit cycle behavior in control systems.[12] Recall that not only does the actuator exhibit hysteresis, but the self-sensing signal does as well.

Conclusions

Implementation of the self-sensing control technique using a magnetostrictive actuator is viable. Results of this Note show that significant damping can be added to a structure. However, the effects of nonlinearities inherent in Terfenol-D make the implementation process nontrivial. A good system estimator would have to be used to implement a proper self-sensing control law. Although seemingly complex, additional self-sensing circuitry would eliminate the need for independent, and potentially noncollocated, sensors. Thus, this proof of concept may motivate actuator designers to consider the potential benefits of self-sensing actuation.

Acknowledgments

The authors would like to express their appreciation to Henry Waites of NASA Marshall Space Flight Center (NASA Grant NGT-50883) and Devendra Garg of the National Science Foundation's Dynamic Systems and Controls Program (Grant MSS9350268).

References

[1]De Boer, E., "Theory of Motional Feedback," *IRE Transaction on Audio*, Vol. AU-9, No. 1, 1961, pp. 15–21.

[2]Dosch, J. J., Inman, D. J., and Garcia, E., "A Self-Sensing Piezoelectric Actuator for Collocated Control," *Journal of Intelligent Material Systems and Structures*, Vol. 3, Jan. 1992, pp. 166–183.

[3]Garcia, E., Dosch, J., and Inman, D. J., "The Application of Smart Structures to the Vibration Suppression Problem," *Journal of Intelligent Material Systems and Structures*, Vol. 3, No. 4, 1992, pp. 659–667.

[4]Jones, L. D., Garcia, E., and Waites, H., "Self-Sensing Control as Applied to a PZT Stack Actuator Used as a Micropositioner," *Smart Materials and Structures*, Vol. 3, No. 2, 1994, pp. 147–156.

[5]Spangler, R. L., and Hall, S. R., "Robust Broadband Control of Flexible Structures Using Integral Piezoelectric Elements," *3rd International Conference on Adaptive Structures* (San Diego, CA), Technomic, Lancaster, PA, 1992, pp. 665–679.

[6]Pratt, J., and Flatau, A., "Development and Analysis of a Self-Sensing Magnetostrictive Actuator Design," *Proceedings of the 1993 SPIE Smart Materials and Structures Conference* (Albuquerque, NM), Vol. 1917, Pt. 2, SPIE, Bellingham, WA, 1993, pp. 952–961.

[7]Fenn, R. C., and Gerver, M. J., "Passive Damping and Velocity Sensing Using Magnetostrictive Transduction," *Proceedings of the SPIE Smart Structures and Materials Conference* (Orlanda, FL), Vol. 2190, SPIE, Bellingham, WA, 1994, pp. 216–227.

[8]De Lacheisserie, E. T., "Magnetostriction of Soft Ferromagnets: Introduction and Theory," *Magnetostriction: Theory and Applications of Magnetoelasticity*, CRC Press, Boca Raton, FL, 1993, pp. 5–8.

[9]Anon., "IEEE Standard on Magnetostrictive Materials: Piezomagnetic Nomenclature," IEEE Std. 319-1990, Inst. of Electrical and Electronics Engineers, New York, 1990.

[10]Anon., "IEEE Standard on Piezoelectricity," ANSI/IEEE Std. 176-1987, Inst. of Electrical and Electronics Engineers, New York, 1987.

[11]Goh, C. J., and Caughey, T. K., "On the Stability Problem Caused by Finite Actuator Dynamics in the Collocated Control of Large Space Structures," *International Journal of Control*, Vol. 41, No. 3, 1985, pp. 787–802.

[12]Ogata, K., "Describing Function Analysis," *Modern Control Engineering*, Prentice–Hall, Englewood Cliffs, NJ, 1970, pp. 645–676.

Precise Trajectory Tracking Control of Elastic Joint Manipulator

Hamza Diken*

Istanbul Technical University, Istanbul 80626, Turkey

I. Introduction

IN the design of high-performance motion systems, the flexibility of the drives and structures, particularly at manipulator arms, presents an obstacle. Some techniques and strategies related to the subject are extensively discussed in Ref. 1.

Similar to the compliance and control of the manipulator arms, a good example of the flexible system is flexible spacecraft, because the location of points at their extremities must be controlled, sometimes to very high precision, by torquing some other point that is separated from the first by sections of flexible structures.[2] In Ref. 3 a survey on the active control technology for large space structures focuses on the development of systematic modeling and design tools for the control of large space structures that has occurred over the past decade.

The objective of this Note is to obtain a transfer function of the servomotor-driven flexible shaft system that includes the natural frequency and damping ratio of the shaft and to propose a trajectory function with which precise trajectory tracking is possible.

The flexible system consists of dc servomotor, harmonic drive, flexible shaft, and manipulator arm. A transfer function relating the actual angular position to the desired angular position of the arm is obtained, including proportional-integral-derivative (PID) type control gains, inductance, flexible system natural frequency, subsystem natural frequency, and the material damping. Transfer function zeros and poles are analyzed in the Laplace domain, and system response to cycloidal input motion is discussed. The close relation between the settling time of the system and the rise time of the trajectory function is presented, and the possibility of the precise tracking of the cycloidal trajectory for the flexible system is shown.

II. Formulation

The flexible system considered here consists of a dc servomotor, harmonic drive, flexible shaft, and a manipulator arm. A sketch of the system is shown in Fig. 1a. Also the equivalent system, at which the motor inertia is reflected to the manipulator arm axis, is shown in Fig. 1b. Here, T indicates torque applied by the dc servomotor, J_m is the motor inertia, θ_m is the motor angular displacement, k and c

---

Received Oct. 14, 1994; revision received Aug. 10, 1995; accepted for publication Nov. 10, 1995.

*Associate Professor, Faculty of Aeronautics and Astronautics, Maslak.

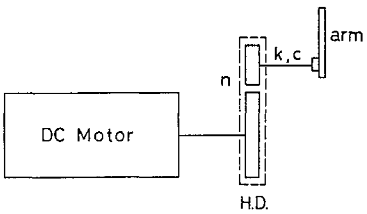

Fig. 1a Dynamic system with flexible shaft.

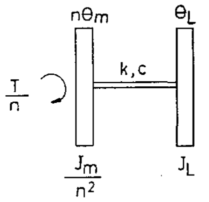

Fig. 1b Equivalent flexible dynamic system.

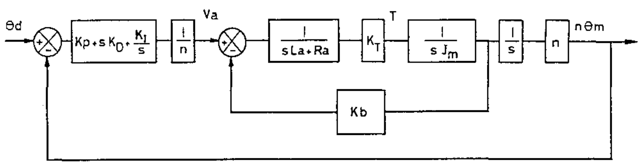

Fig. 2 Closed-loop block diagram of dc servomotor for position control.

are flexible shaft stiffness and damping constant, and θ_L and J_L are arm angle and inertias, respectively. Also, n is the speed reduction ratio of the harmonic drive. For the flexible system shown in Fig. 1b the dynamic equation in matrix form is

$$\begin{bmatrix} J_m/n^2 & 0 \\ 0 & J_L \end{bmatrix}\begin{bmatrix} n\ddot{\theta}_m \\ \ddot{\theta}_L \end{bmatrix}+\begin{bmatrix} c & -c \\ -c & c \end{bmatrix}\begin{bmatrix} n\dot{\theta}_m \\ \dot{\theta}_L \end{bmatrix}$$

$$+\begin{bmatrix} k & -k \\ -k & k \end{bmatrix}\begin{bmatrix} n\theta_m \\ \theta_L \end{bmatrix}=\begin{bmatrix} T/n \\ 0 \end{bmatrix} \tag{1}$$

The Laplace transform of the equation is

$$\begin{bmatrix} n\theta_m \\ \theta_L \end{bmatrix}=\begin{bmatrix} \left[(J_m/n^2)s^2+cs+k\right] & -(cs+k) \\ -(cs+k) & \left(J_L s^2+cs+k\right) \end{bmatrix}^{-1}\begin{bmatrix} T/n \\ 0 \end{bmatrix} \tag{2}$$

A block diagram of the dc servomotor, which is used for the position control of the manipulator arm, is shown in Fig. 2. Here PID control is assumed.[4] In Fig. 2, θ_d is the desired angular displacement; K_P, K_D, and K_I are proportional, derivative, and integral gains; n is the speed reduction ratio; L_a and R_a are motor inductance and resistance; K_T and K_b are torque constant and electromotive force constant; J_m is motor inertia; and θ_m is output of the servomotor. From the block diagram, torque T can be obtained in terms of other parameters as

$$\frac{T}{n}=\frac{K_T[K_P+K_Ds+(K_I/s)]}{n^2(sL_a+R_a)}\theta_d$$

$$-\frac{K_T[K_P+K_Ds+(K_I/s)+K_bs]}{n^2(sL_a+R_a)}n\theta_m \tag{3}$$

When the Eq. (3) is inserted in Eq. (2), the transfer function of the system is obtained as

$$\frac{\theta_L}{\theta_d}=\frac{B(s)}{A(s)}=\frac{b_3s^3+b_2s^2+b_1s+b_0}{a_6s^6+a_5s^5+a_4s^4+a_3s^3+a_2s^2+a_1s+a_0} \tag{4}$$

The polynomials $B(s)$ and $A(s)$ are

$$B(s)=\frac{2\zeta_n}{\omega_n}\frac{1}{T_D}s^3+\left(\frac{2\zeta_n}{\omega_n}\frac{1}{T_P}+\frac{1}{T_D}\right)s^2$$

$$+\left(\frac{2\zeta_n}{\omega_n}\frac{1}{T_I}+\frac{1}{T_P}\right)s+\frac{1}{T_I}$$

$$A(s)=\frac{L_a}{R_a}\frac{1}{\omega_n^2}s^6+\left(\frac{L_a}{R_a}\frac{2\zeta_n}{\omega_n}+\frac{1}{\omega_n^2}\right)s^5+\left[\frac{L_a}{R_a}+\frac{2\zeta_n}{\omega_n}\right.$$

$$\left.+\frac{1}{\omega_n^2}\left(\frac{1}{T_D}+\frac{1}{T_m}\right)\right]s^4+\left[1+\frac{1}{\omega_L^2}\frac{1}{T_P}+\frac{2\zeta_n}{\omega_n}\right.$$

$$\left.\times\left(\frac{1}{T_D}+\frac{1}{T_m}\right)\right]s^3+\left(\frac{1}{\omega_L^2}\frac{1}{T_I}+\frac{2\zeta_n}{\omega_n}\frac{1}{T_P}+\frac{1}{T_D}+\frac{1}{T_m}\right)s^2$$

$$+\left(\frac{2\zeta_n}{\omega_n}\frac{1}{T_I}+\frac{1}{T_P}\right)s+\frac{1}{T_I}$$

where the mechanical time constant of the system is

$$T_m=\frac{R_a\left(J_m+n^2J_L\right)}{K_TK_b} \tag{5}$$

T_P, T_D, and T_I are defined as

$$T_P=\frac{R_a\left(J_m+n^2J_L\right)}{K_TK_P},\qquad T_D=\frac{R_a\left(J_m+n^2J_L\right)}{K_TK_D}$$

$$T_I=\frac{R_a\left(J_m+n^2J_L\right)}{K_TK_I} \tag{6}$$

Undamped natural frequency of the flexible system and the subsystem are

$$\omega_n=\sqrt{\frac{J_m+n^2J_L}{J_mJ_L}k},\qquad \omega_L=\sqrt{\frac{k}{J_L}} \tag{7}$$

When the motor side is fixed, the remaining system is defined as the subsystem. Here, ζ_n is the material damping ratio. Suppose the shaft is rigid; then ω_n and ω_L go to infinity and the transfer function reduces to

$$\frac{\theta_L}{\theta_d}=\left(\frac{1}{T_D}s^2+\frac{1}{T_P}s+\frac{1}{T_I}\right)\Big/\left[\frac{L_a}{R_a}s^4+s^3+\left(\frac{1}{T_D}+\frac{1}{T_m}\right)s^2\right.$$

$$\left.+\frac{1}{T_P}s+\frac{1}{T_I}\right] \tag{8}$$

Suppose $L_a=0$ and torque is not applied to the flexible system (which means $K_T=0$); then the denominator of the transfer function reduces to

$$s^3\left(s^2+2\zeta_n\omega_ns+\omega_n^2\right) \tag{9}$$

which is the characteristic equation for the two-degree-of-freedom dynamic system.

III. Example

To continue the analysis the example given in Table 1 is chosen. All values are taken from Altinay HSR4 model manipulator developed at the KOSGEB facilities of Istanbul Technical University.

L_a appears in Eq. (4), which is generally neglected with respect to R_a. Figures 3 and 4 show the root loci of the system with and without the effect of inductance, respectively. For these plots, gains K_D and K_I and damping ratio ζ_n are set equal to zero. After a certain value of K_P, 318 for the chosen example, inductance causes instability. When material damping is not considered and gains K_D and K_I are set equal to zero, roots start at the poles, which are $-414.83 \pm 336.27j$, $-14.99 \pm 57.31j$, 0.0, 0.0, and end at the zeros, which are $\pm 57.73j$, 0.0, and infinities. To see the effect of the derivative and integral gains, dominant roots close to the imaginary axis are separately plotted in Fig. 5. Root loci near the imaginary axis not clear in Figs. 3 and 4 can be seen in Fig. 5 as the solid line plot. Results show that roots are more sensitive to K_D than to K_I. Increasing values of K_D rapidly lower the real part of the complex roots, and

Table 1 Characteristics of dc servomotor and manipulator arm

$R_a = 4.9\Omega$
$L_a = 5.7$ mH
$K_T = 0.37$ Nm/A
$K_b = 0.37$ Vs/rad
$J_m = 0.8 \times 10^{-4}$ Nms^2
$J_L = 2.4$ Nms^2
$n = 0.01$
$k = 0.8 \times 10^{-4}$ Nm/rad
$\omega_L = 57.73$ rad/s
$\omega_n = 115.47$ rad/s

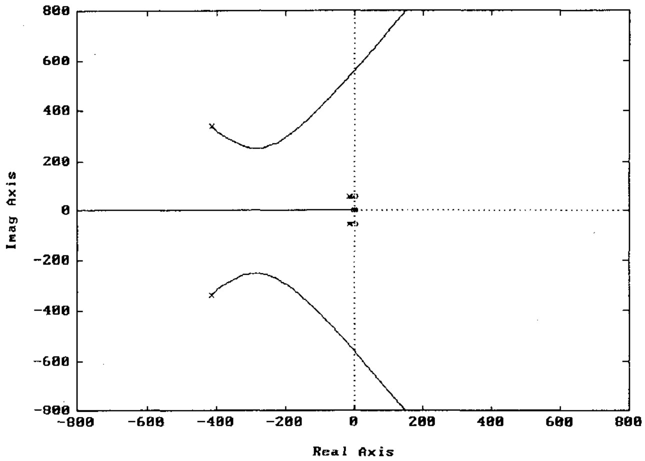

Fig. 3 Root loci when L_a is not neglected.

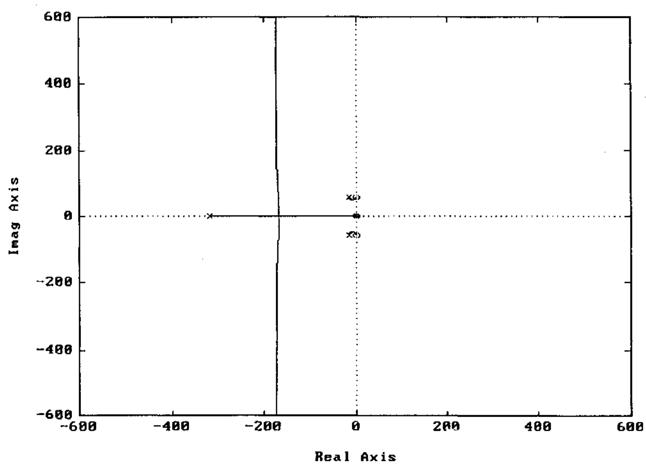

Fig. 4 Root loci when L_a is neglected.

the system becomes more oscillatory. When the system is assumed rigid, the dominant roots, which characterize the system response, do not appear on the root loci plot; therefore, flexibility should be taken into account in the control of dynamic systems.

The manipulator arm is assumed to track the cycloidal trajectory,[5,6] which is given as

$$\theta_d = \Delta\theta\left(\frac{t}{t_r} - \frac{1}{2\pi}\sin 2\pi\frac{t}{t_r}\right) \tag{10}$$

Here $\Delta\theta = \theta_2 - \theta_1$, the angle to be traveled; t_r is the rise time. Let us take the Laplace transform of Eq. (10)

$$\theta_d(s) = \frac{A}{s_2} - \frac{A}{s^2 + \omega_p^2}, \qquad A = \frac{\Delta\theta\omega_p}{2\pi}, \qquad \omega_p = \frac{2\pi}{t_r} \tag{11}$$

Cycloidal motion consists of one ramp and one sinusoidal time function. If the transfer function of the system is type two,[7] then it is expected that the system can follow ramp function without an error. Suppose $K_P = 20$, $K_D = 0.2$, and $K_I = 50$ are selected; then the poles of the transfer function are $-400.72 \pm 514.91j$, $-6.56 \pm 52.24j$, -42.38, -2.70. Dominant roots are $-6.56 \pm 52.24j$, and

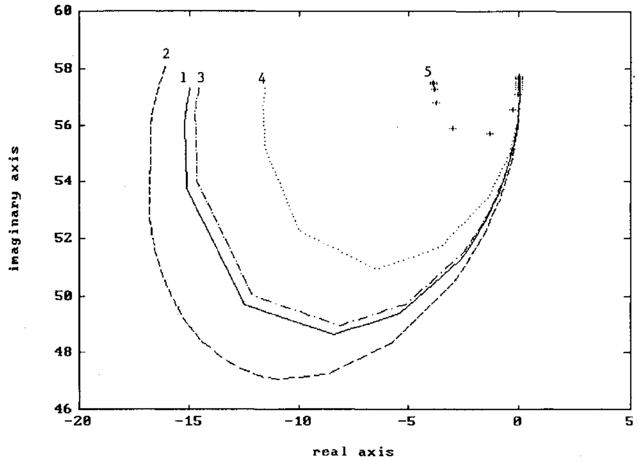

Fig. 5 Root loci of dominant roots: 1) $K_D = 0$, $K_I = 0$; 2) $K_D = 0$, $K_I = 100$; 3) $K_D = 0.01$, $K_I = 0$; 4) $K_D = 0.1$, $K_I = 0$; and 5) $K_D = 1$, $K_I = 0$.

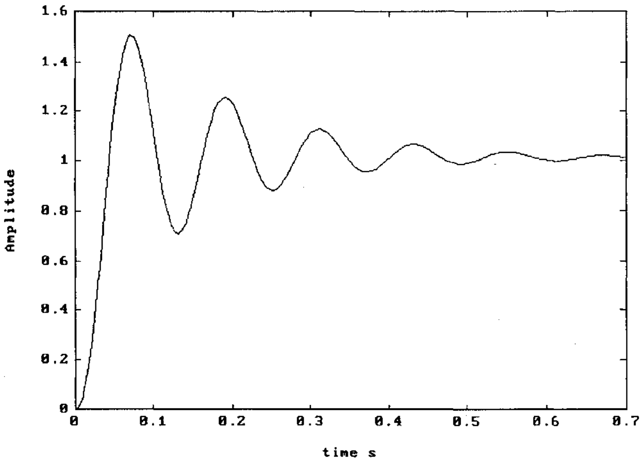

Fig. 6 System response to unit step input.

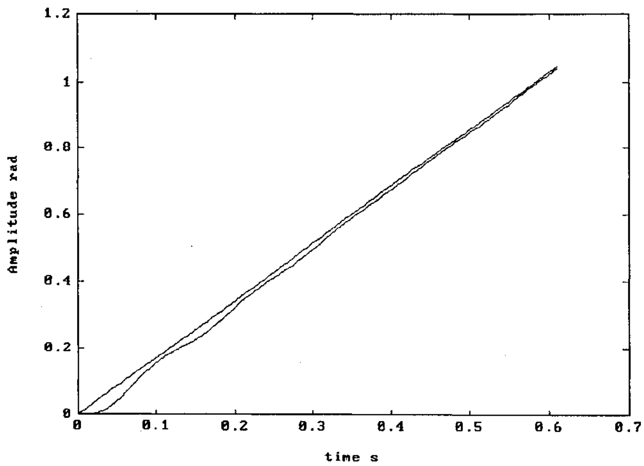

Fig. 7 System response to the ramp part of the cycloidal input.

the system can be considered as a second-order system behaving with these roots. Settling time for the second-order system can be approximated with $t_s = 4/\sigma$ (Ref. 7). Here σ is the real part of the complex root. For the chosen example, $t_s = 0.6098$ s. Figure 6 shows the response of the system to a unit step input. As seen from the figure, assumed settling time t_s is a good approximation for the settling time of the system. Suppose rise time t_r is chosen as equal to settling time t_s of the system; then the response of the system to the ramp part of the cycloidal input is given in Fig. 7. As expected, error is almost zero at $t = t_s = t_r$. But the same t_r is not long enough for the sinusoidal part of the cycloidal input to be followed by the system. The response to the sinusoidal input is seen in Fig. 8. It is observed that $t_r = 4t_s$ is a good approximation for the system to follow the sinusoidal part. For the chosen example, suppose $t_r = 4t_s = 2.439$ s is assumed; the response of the flexible system to the

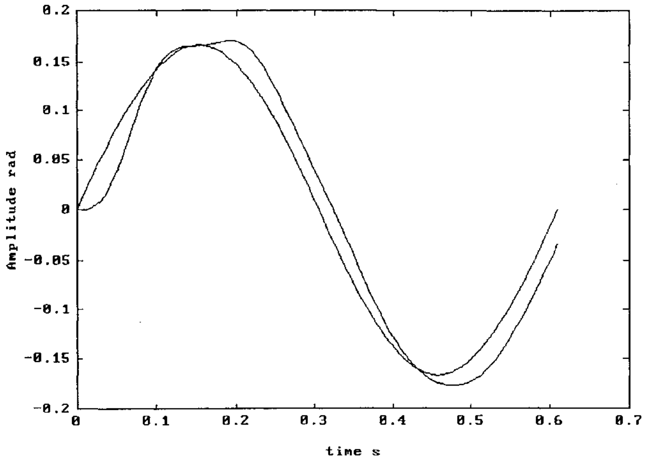

Fig. 8 System response to the sinusoidal part of the cycloidal input.

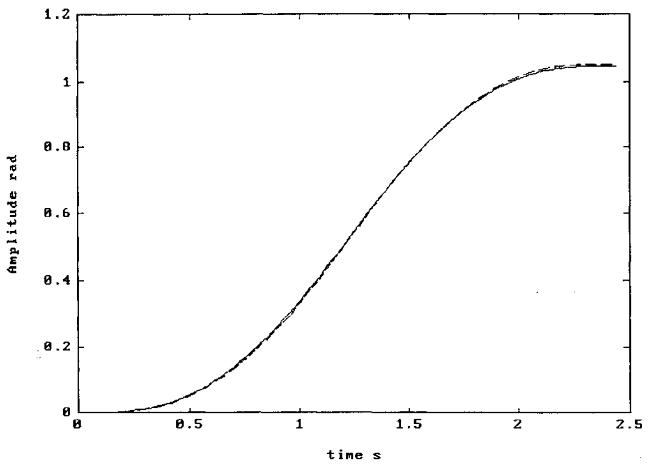

Fig. 9 System response to the cycloidal input function.

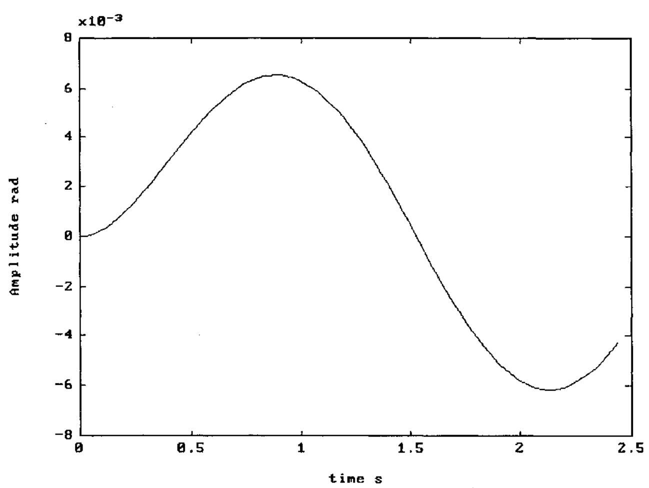

Fig. 10 Tracking error of the flexible system.

cycloidal trajectory and the tracking error are shown in Figs. 9 and 10, respectively. The maximum tracking error is 0.62%. An angular displacement of 1.0472 rad (60 deg) is chosen for the example.

To see the effect of material damping to the system response, $\zeta_n = 0.05$ is assumed; then for previously chosen values of the gains, the system poles are $-405.56 \pm 518.68j$, $-7.56 \pm 51.70j$, -42.25, -2.70. When compared with the poles obtained without material damping, there is little change in system poles and slight increase in the damping of the system, but this does not seriously affect the overall system response.

IV. Conclusion

In this Note a flexible control system consisting of a dc servomotor, harmonic drive, flexible shaft, and manipulator arm is considered. The transfer function of the system relating the manipulator arm angle to the desired trajectory angle is derived, including natural frequencies and material damping of the flexible system, as well as PID gains of the control system. It is shown that the dominant roots of the transfer function, which characterize the response of the flexible system, are totally different from that of a rigid system. Material damping is not very effective on the system response. The flexible system is more sensitive to the derivative gain than to the integral gain. For the chosen particular type of trajectory, which is cycloid, the settling time of the system can be related to the rise time of the cycloid, and precise trajectory tracking can be obtained.

References

[1]Book, W. J., "Controlled Motion in an Elastic World," *Journal of Dynamic Systems, Measurement, and Control*, Vol. 115, June 1993, pp. 252–261.

[2]Cannon, R. H., and Rosenthal, D. E., Jr., "Experiments in Control of Flexible Structure with Noncollocated Sensors and Actuators," *Journal of Guidance, Control, and Dynamics*, Vol. 7, No. 5, 1984, pp. 546–553.

[3]Hyland, D. C., Longman, R. W., and Junkins, J. L., "Active Control Technology for Large Space Structures," *Journal of Guidance, Control, and Dynamics*, Vol. 16, No. 5, 1993, pp. 801–821.

[4]Fu, K. S., Gonzales, R. C., and Lee, C. S. G., *Robotics: Control, Sensing, Vision, and Intelligence*, McGraw–Hill, New York, 1987.

[5]De Luca, A., and Siciliano, B., "Inversion Based Nonlinear Control of Robot Arms with Flexible Links," *Journal of Guidance, Control, and Dynamics*, Vol. 16, No. 6, 1993, pp. 1169–1176.

[6]Shigley, J. E., and Uicker, J. J., *Theory of Machines and Mechanisms*, McGraw–Hill, New York, 1980.

[7]Raven, F. H., *Automatic Control Engineering*, 3rd ed., McGraw–Hill, New York, 1978, p. 409.

Exponential Criterion-Based Guidance Law for Acceleration Constrained Missile and Maneuvering Target

Ilan Rusnak*
RAFAEL, Ministry of Defense, Haifa 31021, Israel

Introduction

THE linear-quadratic (LQ) and linear-quadratic-Gaussian (LQG) theories have been used to derive modern guidance laws. The structure of such modern guidance laws is a guidance gain multiplied by an estimated zero effort miss. The structure for a high-order missile and a maneuvering target is dealt with in Refs. 1 and 2. The guidance gain depends only on the dynamics of the missile. The estimated zero effort miss is the miss without effort, computed with the estimated states. The estimated states are derived by an appropriate Kalman filter. This structure is because of the separation theorem and certainty equivalence principle.[3]

The linear-exponential and linear-exponential-Gaussian (LEG) problems are generalizations of the LQ and LQG problems. The LEG criterion problem has been solved in Ref. 4. It has been applied to homing missile guidance in Ref. 5. The structure of guidance law based on the LEG criterion for a high-order missile and a high-order maneuvering target is treated in Ref. 6. The effect of the acceleration constraint imposed by the structural or aerodynamic limitations on guidance law, based on the LQ and LQG criteria, for a target whose maneuver is described by a high-order transfer function/shaping filter and a high-order, acceleration constrained missile is described in Refs. 7 and 8.

The structure of a guidance law based on exponential criteria for an arbitrary order and acceleration constrained missile and

Received Feb. 20, 1995; revision received Nov. 25, 1995; accepted for publication Nov. 27, 1995.

*Principal Engineer, Department 88, P.O. Box 2250.